Estimation of Amplitude and Phase Parameters of Multicomponent Signals

Benjamin Friedlander, *Fellow, IEEE,* and Joseph M. Francos, *Member, IEEE*

***Abstract*—This paper considers the problem of estimating signals consisting of one or more components of the form $a(t)e^{j\phi(t)}$, where the amplitude and phase functions are represented by a linear parametric model. The Cramér–Rao bound (CRB) on the accuracy of estimating the phase and amplitude parameters is derived. By analyzing the CRB for the single-component case, it is shown that the estimation of the amplitude and the phase are decoupled. Numerical evaluation of the CRB provides further insight into the dependence of estimation accuracy on signal-to-noise ratio (SNR) and the frequency separation of the signal components. A maximum likelihood algorithm for estimating the phase and amplitude parameters is also presented. Its performance is illustrated by Monte-Carlo simulations, and its statistical efficiency is verified.**

I. Introduction

MANY signals used in communications, sonar, radar, and other engineering systems, as well as various natural signals, involve amplitude and/or frequency modulation of a carrier. The complex (analytic signal) representation of such signals is given by $s(t) = a(t)e^{j\phi(t)}$, where $a(t)$ and $\phi(t)$ are the amplitude and phase functions. Signals with a more complicated structure can be represented by a combination of signals of this type. In the following, we refer to signals as being either single-component or multicomponent signals, where the word "component" refers to a term of the form $a(t)e^{j\phi(t)}$.

It should be noted that in general the decomposition of a signal into components of these type is not unique. Conditions under which a unique representation is available are discussed in [1], and in the following, we will consider only signals of this type. In essence, we assume that each signal component has a small instantaneous bandwidth and that the different components are well separated in the time-frequency plane. See also [2]–[5] for a discussion of time-frequency representations and the notions of instantaneous frequency and bandwidth.

Current approaches to the analysis of such signals focus on nonparametric time-frequency distributions. The technique proposed in this paper provides an alternative parametric approach (see also [18]). Since the suggested method is parametric, it alleviates the well known problems of nonparametric time-frequency distributions such as time-frequency resolution, cross-terms, etc.

Consider the problem of estimating multicomponent signals in the presence of additive white Gaussian noise. The approach we take is to assume a linear parametric model for the amplitude and phase functions and to estimate these parameters from the available data. In other words, the amplitude and the phase of each signal component are assumed to be a linear combination of some known functions of time (referred to as basis functions), where the coefficients associated with each function are some unknown constants. Given noisy observations of the signal over a finite interval, we wish to estimate these unknown coefficients. In Section III, we derive the maximum likelihood estimator (MLE) for the signal parameters. In Section IV, we develop the Cramér–Rao bound (CRB) for the covariance of the estimation errors, which provides a well-known lower-bound for the achievable variance of any unbiased estimator of these parameters. The bound is derived both for the amplitude and phase parameters, and for the amplitude and phase functions. In Section V, we present some numerical examples that illustrate the performance of the maximum likelihood estimator and verify its statistical efficiency when the signal-to-noise ratio (SNR) is sufficiently high. We note that the emphasis in this paper is on the performance analysis of parameteric amplitude and phase estimation and not on algorithmic issues. We introduced the ML algorithm primarily for the purpose of verifying by simulation our analytical results.

The analysis of the CRB for the single-component case yields some interesting results. In Section IV, we show that the estimation of the amplitude and the phase are decoupled in this case, i.e., the corresponding Fisher information matrix (FIM) has a block diagonal structure. It is also shown that the CRB for the amplitude parameters depends only on the basis functions for the amplitude and is independent of both the amplitude parameter values and of the phase of the signal. Furthermore, the CRB for the phase parameters depends on the amplitude waveform and the basis functions for the phase but does not depend explicitly on either the phase or the choice of the parametric model for the amplitude function.

The analysis presented in this paper generalizes some previously published results. The problem of estimating the phase parameters of a single-component constant amplitude signal has been studied in [6] and [7] for the special case where the phase is assumed to be a polynomial function of time. Peleg *et al.* [6], [7] derive a computationally efficient

Manuscript received June 12, 1993; revised September 21, 1994. This work was supported by the Army Research Office under contract no. DAAL03-91-C-0022 and the U.S. Army Communications Electronics Command, Center for Signals Warfare. The associate editor coordinating the review of this paper and approving it for publication was Prof. John Goutsias.

B. Friedlander is with the Department of Electrical and Computer Engineering, University of California, Davis, CA 95616 USA.

J. M. Francos is with the Department of Electrical and Computer Engineering, Ben-Gurion University, Beer Sheva, Israel.

IEEE Log Number 9409780.

1053-587X/95$04.00

suboptimal estimation technique for the phase parameters, using the polynomial phase transform. In [8] and [9], this work is generalized to multicomponent signals, where each component has a constant amplitude and polynomial phase. Different approaches to estimating the phase parameters of multicomponent constant amplitude signals are presented in [10] and [11]. Results for the joint estimation of both amplitude and phase parameters do not seem to have been published before.

II. Problem Formulation

In this section, we describe the problem to be treated in this paper. Let $\{y(t)\}$ be a discrete time process consisting of the sum of a deterministic signal and additive white Gaussian noise. More specifically

$$y(t) = \sum_{i=1}^{I} s_i(t) + n(t) \qquad t = 0, 1, \cdots, M \tag{1}$$

where I is the *a priori* known number of components of the observed signal. Each of the components is of the general form

$$s_i(t) = a_i(t) e^{j\phi_i(t)} \tag{2}$$

where $a_i(t)$ is the amplitude of the ith signal and $\phi_i(t)$ is its phase. Let the amplitude of the ith signal be given by

$$a_i(t) = \sum_{k=0}^{P_i} a_{i,k} \rho_{i,k}(t) \tag{3}$$

and similarly, let the phase be given by

$$\phi_i(t) = \sum_{\ell=0}^{Q_i} b_{i,\ell} \eta_{i,\ell}(t) \tag{4}$$

where the model parameters, $\{a_{i,k}\}, \{b_{i,\ell}\}$ are real valued, while $\{\rho_{i,k}(t)\}$ and $\{\eta_{i,\ell}(t)\}$ are some arbitrary sets of real valued basis functions, which may be different for each component. The observation noise $n(t)$ is assumed to be a complex, zero-mean white Gaussian noise of unknown variance.

Define

$$\boldsymbol{y} = [y(0), y(1), \cdots, y(M)]^T \tag{5}$$

$$\boldsymbol{a}_i = [a_{i,0}, a_{i,1}, \cdots, a_{i,P_i}]^T \tag{6}$$

and let all of the amplitude parameters be assembled in a vector $\boldsymbol{a}$

$$\boldsymbol{a} = [\boldsymbol{a}_1^T, \boldsymbol{a}_2^T, \cdots, \boldsymbol{a}_I^T]^T. \tag{7}$$

Similarly, let

$$\boldsymbol{b}_i = [b_{i,0}, b_{i,1}, \cdots, b_{i,Q_i}]^T \tag{8}$$

and let all of the phase parameters be assembled into a vector $\boldsymbol{b}$

$$\boldsymbol{b} = [\boldsymbol{b}_1^T, \boldsymbol{b}_2^T, \cdots, \boldsymbol{b}_I^T]^T. \tag{9}$$

Also let

$$\boldsymbol{t} = [0, 1, \cdots, M]^T. \tag{10}$$

In the following, we will use the following shorthand vector notation for functions of time. Given a scalar function $f(t)$, we will denote the column vector consisting of the values of $f(t),\ t = 1, \cdots, M$ by $f(\boldsymbol{t})$.

Using this notation, we denote the vector of phase values of the ith signal by $\phi_i(\boldsymbol{t})$. Similarly, the vector of the basis function $\rho_{i,k}(t)$ values is denoted by $\rho_{i,k}(\boldsymbol{t})$. Hence, we can write

$$\boldsymbol{\Phi}_i = [\rho_{i,0}(\boldsymbol{t}) \cdot e^{j\phi_i(\boldsymbol{t})}, \rho_{i,1}(\boldsymbol{t}) \cdot e^{j\phi_i(\boldsymbol{t})}, \rho_{i,2}(\boldsymbol{t}) \cdot e^{j\phi_i(\boldsymbol{t})}, \cdots, \rho_{i,P_i}(\boldsymbol{t}) \cdot e^{j\phi_i(\boldsymbol{t})}] \tag{11}$$

where $\cdot$ denotes element by element multiplication of the entries of the vectors, and $e^{j\phi_i(\boldsymbol{t})}$ is an $M+1$ dimensional column vector. We therefore have

$$\boldsymbol{\Phi} = [\boldsymbol{\Phi}_1, \boldsymbol{\Phi}_2, \cdots, \boldsymbol{\Phi}_I]. \tag{12}$$

Using the above definitions, we can rewrite (1) in the following matrix representation:

$$\boldsymbol{y} = \boldsymbol{\Phi a} + \boldsymbol{n}. \tag{13}$$

Note that $\boldsymbol{y}$ is a linear function of the amplitude parameters $\boldsymbol{a}$, while the phase parameters enter nonlinearly through $\boldsymbol{\Phi}$.

The estimation problem considered in this paper can now be formulated as follows. Given the observations $\{y(t)\}_{t=0}^{M}$, where $M > \sum_i ((P_i + 1) + (Q_i + 1))$, estimate the phase and amplitude parameters $\boldsymbol{b}, \boldsymbol{a}$. Then, use the estimated parameters to form an estimate of the amplitudes and phases of the signal components by inserting the estimated parameters into (3) and (4).

III. The Maximum Likelihood Estimator

In this section, we derive the MLE for the problem defined above and describe briefly its implementation.

Since the observation noise is assumed to be a white Gaussian process, the probability density function of the observations is given by

$$p(\boldsymbol{y}; \boldsymbol{\theta}) = \frac{1}{(\pi\sigma^2)^{M+1}} \exp\left\{-\frac{1}{\sigma^2}\|\boldsymbol{y} - \boldsymbol{\Phi a}\|^2\right\} \tag{14}$$

where $\boldsymbol{\theta} = [\boldsymbol{b}^T \boldsymbol{a}^T]^T$ denotes the vector of unknown parameters. The log-likelihood function Λ is then given by

$$\Lambda = -(M+1)\ln \pi - (M+1)\ln \sigma^2 - \frac{1}{\sigma^2}\|\boldsymbol{y} - \boldsymbol{\Phi a}\|^2. \tag{15}$$

Let $\tilde{\boldsymbol{y}} = [\mathrm{Re}\{\boldsymbol{y}\}^T, \mathrm{Im}\{\boldsymbol{y}\}^T]^T$, and let $\boldsymbol{\Psi} = [\mathrm{Re}\{\boldsymbol{\Phi}\}^T, \mathrm{Im}\{\boldsymbol{\Phi}\}^T]^T$. We can then rewrite the log-likelihood function using real quantities only as

$$\Lambda = -(M+1)\ln \pi - (M+1)\ln \sigma^2 - \frac{1}{\sigma^2}\|\tilde{\boldsymbol{y}} - \boldsymbol{\Psi a}\|^2. \tag{16}$$

The MLE of the signal parameters is found by minimizing Λ over the amplitude and the phase parameters. Because of the fact that the log-likelihood function is a quadratic function of the amplitude parameters, the minimization over $\boldsymbol{a}$ can be carried out analytically for any given value of $\boldsymbol{b}$. It is straightforward to show that

$$\hat{\boldsymbol{a}} = (\boldsymbol{\Psi}^T\boldsymbol{\Psi})^{-1}\boldsymbol{\Psi}^T\tilde{\boldsymbol{y}} \tag{17}$$

will minimize Λ over $\boldsymbol{a}$. By inserting (17) into (16) we get

$$\overline{\Lambda} = -(M+1)\ln \pi - (M+1)\ln \sigma^2 - \frac{1}{\sigma^2}J(\boldsymbol{b}) \quad (18)$$

where $\overline{\Lambda}$ is the likelihood function with $\boldsymbol{a}$ replaced by $\hat{\boldsymbol{a}}$, and

$$J(\boldsymbol{b}) = \tilde{\boldsymbol{y}}^T \boldsymbol{P}_{\boldsymbol{\Psi}}^{\perp} \tilde{y} \quad (19)$$

$$\boldsymbol{P}_{\boldsymbol{\Psi}} = \boldsymbol{\Psi}(\boldsymbol{\Psi}^T\boldsymbol{\Psi})^{-1}\boldsymbol{\Psi}^T \quad (20)$$

$$\boldsymbol{P}_{\boldsymbol{\Psi}}^{\perp} = \boldsymbol{I} - \boldsymbol{\Psi}(\boldsymbol{\Psi}^T\boldsymbol{\Psi})^{-1}\boldsymbol{\Psi}^T. \quad (21)$$

Here, $\boldsymbol{P}_{\boldsymbol{\Psi}}$ and $\boldsymbol{P}_{\boldsymbol{\Psi}}^{\perp}$ denote the projection matrices on the signal and noise subspaces. The signal space is spanned by the columns of $\boldsymbol{\Psi}$, and the orthogonal complement of that subspace is called the noise subspace.

Thus, maximization of the likelihood function is achieved by minimizing the objective function $J(\boldsymbol{b})$, which is a function only of the phase parameters. We have thus shown that the original minimization problem (16) is *separable* since its solution can be reduced to a minimization problem in the nonlinear parameters $\boldsymbol{b}$ only, while $\boldsymbol{a}$ can then be determined by solving a linear least squares problem. Since $J(\boldsymbol{b})$ is a nonlinear function of the phase parameters, this optimization problem cannot be solved analytically, and we must resort to numerical methods. In order to avoid the enormous computational burden of an exhaustive search, we used the following two-step procedure.

In the first step, we obtain an initial estimate for the phase parameters using a suboptimal estimation technique based on the polynomial phase transform [8], [9]. In the second step, we refine these initial estimates by an iterative numerical minimization of the objective function $J(\boldsymbol{b})$. In our experiments, we used the BFGS quasi-Newton optimization method [14], [15]. This algorithm requires evaluation of the first derivative of the objective function at each iteration. An analytic expression for the derivative is derived in the Appendix. As is well known, this type of iterative optimization procedure converges to a local minimum and does not guarantee global optimality, unless the initial estimate is sufficiently close to the global optimum. As we show in Section V, the initial estimates provided by the polynomial phase transform based estimator appear to provide a good initial starting point (i.e., one that leads to convergence to the global minimum) when the SNR is sufficiently high. The performance of the ML algorithm is discussed in more detail in Section V and is compared with the CRB derived in the next section.

The general framework of separable minimization problems is discussed in [12] and [13]. In [12], implementations of the Gauss–Newton, Gauss–Newton–Marquardt, and Davidon–Fletcher–Powell algorithms for minimizing the reduced nonlinear objective function are developed. The performance of the algorithms is then compared with their performance as they operate on the original problem, and it is concluded that the convergence of the minimization algorithm is generally faster when the reduced objective function is minimized rather than the full functional. The test problems in [12] are the parameter estimation of a sum of exponentials, and the parameter estimation of a sum of Gaussians with an exponential background, which are different from the problem discussed in the present paper. Nevertheless, in the present paper, we use a similar approach of employing the separability of our problem in order to minimize, by using a standard algorithm, a reduced nonlinear objective function rather than the full functional. The method presented in [13] is a generalization of Prony's method to general least squares separable problems. It is shown that by using a specific transformation, separable nonlinear least squares cost functions can be split into a sum of quadratic forms in a way that eliminates the linear parameters of the original minimization problem. The method of [12] is shown to be a special case that results from a specific selection of the transformation matrix. An improved method for selecting the transformation is given, and used to derive an algorithm for solving the problem of exponential fitting by reducing it to a minimization problem subject to a single equality constraint.

In the earlier discussion, we assumed that the noise variance σ^2 is known. If it is not known, it can be estimated. The MLE of σ^2 is derived by differentiating the log-likelihood function in (16) with respect to σ^2 and setting the derivative to zero. This yields

$$\frac{\partial \Lambda}{\partial \sigma^2} = -\frac{(M+1)}{\sigma^2} + \frac{1}{\sigma^4}J(\boldsymbol{b}) = 0 \quad (22)$$

and it follows that

$$\hat{\sigma}^2 = \frac{1}{M+1}J(\hat{\boldsymbol{b}}). \quad (23)$$

Thus, the estimation of the noise variance is straightforward, once the MLE's of the other parameters are available.

IV. The Cramer–Rao Bound

In this section, we derive the CRB for the amplitude and phase parameters and the noise variance. We use the well-known formula that states that the elements of the FIM are given by

$$\boldsymbol{F}_{ij} = -E\left\{\frac{\partial^2 \Lambda}{\partial \theta_i \partial \theta_j}\right\} \quad (24)$$

and the CRB is simply the inverse of the FIM [16]. Thus, to evaluate the FIM we need to compute the derivatives of the log-likelihood function with respect to the various parameters of interest, and take their expected value.

A. Computation of the Derivatives

Taking the partial derivative of Λ, we have

$$\begin{aligned}\frac{\partial \Lambda}{\partial b_{i,k}} &= \frac{1}{\sigma^2}\left\{\boldsymbol{a}^H \frac{\partial \boldsymbol{\Phi}^H}{\partial b_{i,k}}(\boldsymbol{y} - \boldsymbol{\Phi a}) + (\boldsymbol{y} - \boldsymbol{\Phi a})^H \frac{\partial \boldsymbol{\Phi}}{\partial b_{i,k}}\boldsymbol{a}\right\} \\ &= \frac{2}{\sigma^2}\,\mathrm{Re}\left\{\boldsymbol{a}^H \frac{\partial \boldsymbol{\Phi}^H}{\partial b_{i,k}}(\boldsymbol{y} - \boldsymbol{\Phi a})\right\} \\ &= \frac{2}{\sigma^2}\,\mathrm{Re}\left\{\boldsymbol{a}_i^H \frac{\partial \boldsymbol{\Phi}_i^H}{\partial b_{i,k}}(\boldsymbol{y} - \boldsymbol{\Phi a})\right\}. \end{aligned} \quad (25)$$

The last equality follows from the identity

$$\frac{\partial \boldsymbol{\Phi}}{\partial b_{i,k}} = \left[\boldsymbol{0}, \cdots, \boldsymbol{0}, \frac{\partial \boldsymbol{\Phi}_i}{\partial b_{i,k}}, \boldsymbol{0}, \cdots, \boldsymbol{0}\right]. \quad (26)$$

Hence, for all i, j

$$-E\left\{\frac{\partial^2\Lambda}{\partial b_{i,k}\partial b_{j,n}}\right\} = \frac{2}{\sigma^2}\,\mathrm{Re}\left\{\boldsymbol{a}_i^H \frac{\partial \boldsymbol{\Phi}_i^H}{\partial b_{i,k}} \frac{\partial \boldsymbol{\Phi}_j}{\partial b_{j,n}} \boldsymbol{a}_j\right\} = \frac{2}{\sigma^2}\,\mathrm{Re}\left\{\tilde{\boldsymbol{a}}_{i,k}^H \tilde{\boldsymbol{a}}_{j,n}\right\} \tag{27}$$

where we define

$$\tilde{\boldsymbol{a}}_{j,n} = \frac{\partial \boldsymbol{\Phi}_j}{\partial b_{j,n}} \boldsymbol{a}_j, n = 0, \cdots, Q_j, \qquad j = 1, \cdots, I. \tag{28}$$

Let $\boldsymbol{u}_{s(i,n)}$ be a $\Sigma_{m=1}^{I}(P_m + 1)$ dimensional column vector whose $s(i,n)$th element equals one, where $s(i,n) = \Sigma_{m=1}^{i-1}(P_m + 1) + (n + 1)$. All other elements are zero. Using this notation, we have

$$\frac{\partial \Lambda}{\partial a_{i,n}} = \frac{2}{\sigma^2}\,\mathrm{Re}\,\{\boldsymbol{u}_{s(i,n)}^H \boldsymbol{\Phi}^H(\boldsymbol{y} - \boldsymbol{\Phi a})\}. \tag{29}$$

$$-E\left\{\frac{\partial^2\Lambda}{\partial b_{j,k}\partial a_{i,n}}\right\} = \frac{2}{\sigma^2}\,\mathrm{Re}\left\{\boldsymbol{a}_j^H \frac{\partial \boldsymbol{\Phi}_j^H}{\partial b_{j,k}} \boldsymbol{\Phi u}_{s(i,n)}\right\} = \frac{2}{\sigma^2}\,\mathrm{Re}\,\{\tilde{\boldsymbol{a}}_{j,k}^H \boldsymbol{\Phi}_{i_{n+1}}\} \tag{30}$$

where $\boldsymbol{\Phi}_{i_{n+1}}$ is the $(n+1)$ column of $\boldsymbol{\Phi}_i$. Similarly

$$-E\left\{\frac{\partial^2\Lambda}{\partial a_{j,k}\partial a_{i,n}}\right\} = \frac{2}{\sigma^2}\,\mathrm{Re}\,\{\boldsymbol{u}_{s(i,n)}^H \boldsymbol{\Phi}^H \boldsymbol{\Phi u}_{s(j,k)}\} = \frac{2}{\sigma^2}\,\mathrm{Re}\,\{\boldsymbol{\Phi}_{i_{n+1}}^H \boldsymbol{\Phi}_{j_{k+1}}\}. \tag{31}$$

Let

$$\boldsymbol{A}_i = [\tilde{\boldsymbol{a}}_{i,0}, \tilde{\boldsymbol{a}}_{i,1}, \cdots, \tilde{\boldsymbol{a}}_{i,Q_i}], \qquad i = 1, \cdots, I, \tag{32}$$

$$\boldsymbol{A} = [\boldsymbol{A}_1, \boldsymbol{A}_2, \cdots, \boldsymbol{A}_I]. \tag{33}$$

A more explicit expression for $\boldsymbol{A}_i$ can be obtained by noting that (28) gives

$$\begin{aligned}\tilde{\boldsymbol{a}}_{i,n} &= \frac{\partial \boldsymbol{\Phi}_i}{\partial b_{i,n}} \boldsymbol{a}_i \\ &= j\eta_{i,n}(\boldsymbol{t}) \cdot \boldsymbol{\Phi}_i \boldsymbol{a}_i \\ &= j\eta_{i,n}(\boldsymbol{t}) \cdot a_i(\boldsymbol{t}) \cdot e^{j\phi_i(\boldsymbol{t})} \\ &= j\eta_{i,n}(\boldsymbol{t}) \cdot s_i(\boldsymbol{t}), \qquad n = 0, \cdots, Q_i, \\ &\qquad i = 1, \cdots, I\end{aligned} \tag{34}$$

where $a_i(\boldsymbol{t})$ and $s_i(\boldsymbol{t})$ are the vectors of the amplitude and signal values of the ith component at each time instant t. Substituting (34) to (32), we have

$$\boldsymbol{A}_i = j[\eta_{i,0}(\boldsymbol{t}) \cdot s_i(\boldsymbol{t}), \eta_{i,1}(\boldsymbol{t}) \cdot s_i(\boldsymbol{t}), \cdots, \eta_{i,Q_i}(\boldsymbol{t}) \cdot s_i(\boldsymbol{t})] \quad i = 1, \cdots, I. \tag{35}$$

Combining the results above, we can write the FIM as

$$-E\left\{\frac{\partial^2\Lambda}{\partial \boldsymbol{\theta}^2}\right\} = \frac{2}{\sigma^2}\,\mathrm{Re}\,\{[\boldsymbol{A}, \boldsymbol{\Phi}]^H[\boldsymbol{A}, \boldsymbol{\Phi}]\}. \tag{36}$$

The CRB for $\boldsymbol{\theta}$ is the inverse of this matrix.

In the case where the noise variance is unknown, the FIM needs to be augmented by a row and a column corresponding to derivatives with respect to σ^2. Using (25), we obtain

$$-E\left\{\frac{\partial^2\Lambda}{\partial b_{i,k}\partial \sigma^2}\right\} = 0. \tag{37}$$

Similarly, using (29)

$$-E\left\{\frac{\partial^2\Lambda}{\partial a_{i,n}\partial \sigma^2}\right\} = 0. \tag{38}$$

Finally

$$-E\left\{\frac{\partial^2\Lambda}{\partial^2 \sigma^2}\right\} = \frac{M+1}{\sigma^4}. \tag{39}$$

Since the FIM is block diagonal, the CRB for the estimate of σ^2 is decoupled from the CRB of $\boldsymbol{\theta}$ and is simply

$$\mathrm{CRB}(\sigma^2) = \frac{\sigma^4}{M+1}. \tag{40}$$

From (36), we note that the FIM for the phase and amplitude parameters is a function of the signal components $s_i(t)$, their phases $\phi_i(t)$ and the phase and amplitude basis functions $\rho_i(t), \eta_i(t)$. Thus, the FIM is independent of $\boldsymbol{a}$ and $\boldsymbol{b}$. It depends on the phase and amplitude parameters only through the phase and amplitude functions.

B. Bounds for the Amplitude, Phase, and Frequency

In many cases we are interested not in the phase or amplitude parameters, but in estimating the signal or its individual components. Having estimated $\boldsymbol{a}, \boldsymbol{b}$, we can estimate the signal amplitude and phase functions simply by inserting the estimated parameters into the assumed signal model. In other cases, we may be interested in estimating the instantaneous frequency of the signal components, which can be computed in a straightforward manner by evaluating the derivative of the phase function. In the following, we derive the CRB for the signal amplitudes, phases, and instantaneous frequencies. Since all of these quantities are functions of the estimated parameters, we will use the following generalized form of the CRB.

Let β be a continuous and differentiable function of the parameter vector $\boldsymbol{\theta}$, i.e., $\beta = f(\boldsymbol{\theta})$. Then, the CRB for β is related to the CRB of $\boldsymbol{\theta}$ by

$$\mathrm{CRB}(\beta) = (\boldsymbol{f}')^T \mathrm{CRB}(\boldsymbol{\theta}) \boldsymbol{f}' \tag{41}$$

where the column vector f' is defined by

$$\boldsymbol{f}' = \frac{\partial f}{\partial \boldsymbol{\theta}}. \tag{42}$$

See, e.g., [17]. Using this formula, the CRB for the desired functions can be computed in a straightforward manner.

The instantaneous phase is defined in (4) as a linear vector function of $\boldsymbol{b}$. The CRB on the phase of the ith signal is, therefore, given by

$$\mathrm{CRB}(\phi_i(t)) = \boldsymbol{g}_i^T \mathrm{CRB}(\boldsymbol{b}_i) \boldsymbol{g}_i, \tag{43}$$

where

$$\boldsymbol{g}_i^T = \left[\frac{\partial \phi_i}{\partial b_{i,0}}, \cdots, \frac{\partial \phi_i}{\partial b_{i,Q_i}}\right] = [\eta_{i,0}(t), \eta_{i,1}(t), \cdots, \eta_{i,Q_i}(t)]. \quad (44)$$

Similarly, the CRB on the instantaneous amplitude of the ith signal is

$$\mathrm{CRB}(a_i(t)) = \boldsymbol{f}_i^T \mathrm{CRB}(\boldsymbol{a}_i)\boldsymbol{f}_i \quad (45)$$

where

$$\boldsymbol{f}_i^T = \left[\frac{\partial a_i}{\partial a_{i,0}}, \cdots, \frac{\partial a_i}{\partial a_{i,P_i}}\right] = [\rho_{i,0}(t), \rho_{i,1}(t), \cdots, \rho_{i,P_i}(t)]. \quad (46)$$

The instantaneous frequency is the time derivative of the instantaneous phase

$$\omega_i(t) = \frac{1}{2\pi}\phi_i'(t) = \frac{1}{2\pi}\sum_{\ell=0}^{Q_i} b_{i,\ell}\eta_{i,\ell}'(t) \quad (47)$$

and therefore

$$\mathrm{CRB}(\omega_i(t)) = \boldsymbol{h}_i^T \mathrm{CRB}(\boldsymbol{b}_i)\boldsymbol{h}_i \quad (48)$$

where

$$\boldsymbol{h}_i^T = \left[\frac{\partial \omega_i}{\partial b_{i,0}}, \cdots, \frac{\partial \omega_i}{\partial b_{i,Q_i}}\right] = \frac{1}{2\pi}[\eta_{i,0}'(t), \eta_{i,1}'(t), \cdots, \eta_{i,Q_i}'(t)]. \quad (49)$$

C. The Single Component Case

Consider the special case where the signal consists of a single component, i.e., the case where $I = 1$. In this case, $\boldsymbol{A}^H\boldsymbol{\Phi} = \boldsymbol{A}_1^H\boldsymbol{\Phi}_1$ is purely imaginary and $\mathrm{Re}\{\boldsymbol{A}^H\boldsymbol{\Phi}\} = 0$. Therefore, the FIM in (36) is block diagonal, and the CRB's on the estimation of the amplitude and phase parameters are decoupled. In other words

$$\mathrm{CRB}(\boldsymbol{a}_1) = \frac{\sigma^2}{2}\{\boldsymbol{\Phi}^H\boldsymbol{\Phi}\}^{-1} \quad (50)$$

and

$$\mathrm{CRB}(\boldsymbol{b}_1) = \frac{\sigma^2}{2}\{\boldsymbol{A}^H\boldsymbol{A}\}^{-1}. \quad (51)$$

The decoupling of the CRB holds for any parameterization of amplitude and phase functions in the single component case. Intuitively, the decoupling exists since in the single component case, no interference with other components occurs.

Note that $\boldsymbol{\Phi}^H\boldsymbol{\Phi}$ is a function of the basis functions $\{\rho_{1,i}(t)\}$ only and is independent of the amplitude and phase parameters or waveforms. In other words, the CRB of the amplitude parameters depends only on the class of functions to which the amplitude function belongs, and is independent of the phase waveform or model. For example, if we represent the amplitude as a polynomial function of time, all signals whose amplitude is a P_1-th order polynomial of time, will have the same values of $\mathrm{CRB}(\boldsymbol{a}_1)$.

Similarly, $\boldsymbol{A}^H\boldsymbol{A}$ is a function of the basis functions $\{\eta_{1,n}(t)\}$ and of the amplitude function $a_1(t)$. In other words, the CRB of the phase parameters does not depend on the parametric model used for the amplitude function and depends only on the class of functions to which the phase function belongs but does not depend on the values of the phase parameters. For example, if we represent the phase as a polynomial function of time, all signals whose phase is a Q_1-th order polynomial of time, and which have the same amplitude function $a_1(t)$, will have the same values of $\mathrm{CRB}(\boldsymbol{b}_1)$.

The results above can be used to gain some insight into the problem of estimating the phase of the signal without assuming a parametric model for the amplitude. In this case, $\boldsymbol{a}$ is specified by the samples of the amplitude function

$$\boldsymbol{a} = [a(0), a(1), \cdots, a(M)]^T. \quad (52)$$

Note that the estimation of $M+1$ amplitude parameters and Q_1 phase parameters from only $M+1$ data points is possible since the data is complex (equivalent to $2(M+1)$ real data points), while the estimated parameters are real. Thus, the nonparametric estimation of the amplitude function leads to a well-posed estimation problem in the single component case (but not if there is more than one component).

From the earlier discussion, it follows that the CRB for the phase parameters is the same in this case as in the case where we assumed a parametric model for the amplitude since $\mathrm{CRB}(\boldsymbol{b}_1)$ depends only on $\{\eta_{1,n}(t)\}$ and on the amplitude function $a_1(t)$. Similar comments apply to the instantaneous phase (IP) and the instantaneous frequency (IF) of the signal, which are functions of the phase parameters. In other words, the accuracy of the IF and IP estimates is independent of whether or not we use a parametric model for the amplitude of the signal.

V. Numerical Examples

In this section, we present some numerical examples in which we evaluate the CRB that was derived in Section IV and perform parameter estimation using the maximum likelihood algorithm presented in Section III.

A. The CRB for Multicomponent Signals

In the case of a multicomponent signal, the FIM is no longer block diagonal in general, and the elements of the off-diagonal blocks are functions of the phase differences between pairs of signal components, their amplitude waveforms, and the amplitude and phase basis functions. To gain some insight into the behavior of the bound we must resort to numerical evaluation of specific examples. Here, we consider the case where both the amplitude and the phase functions are polynomial functions of time, and we consider some interesting special cases. In all the examples presented in this section, the white Gaussian observation noise is of unit variance, the time axis shows the sampling time, and the samples are equispaced.

Example 1: Consider the case of a two-component signal comprised of two linear chirp components: Component #1 has a quadratic amplitude, while component #2 is of a constant amplitude. The instantaneous frequencies of the signal's components are depicted in Fig. 1. Two cases are discussed.

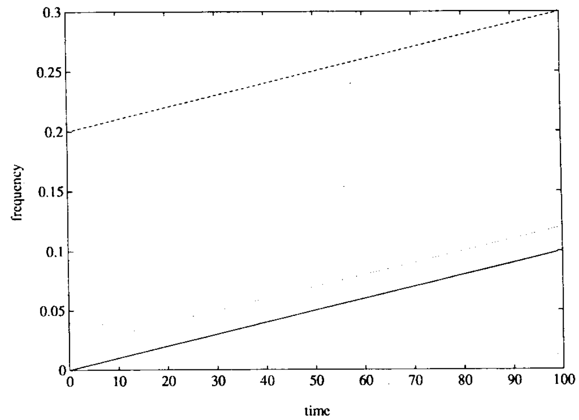

Fig. 1. Instantaneous frequencies of the two-component signal in Example 1: Component #1 (solid line), component #2 in Case I (dashed line), and component #2 in Case II (dotted line).

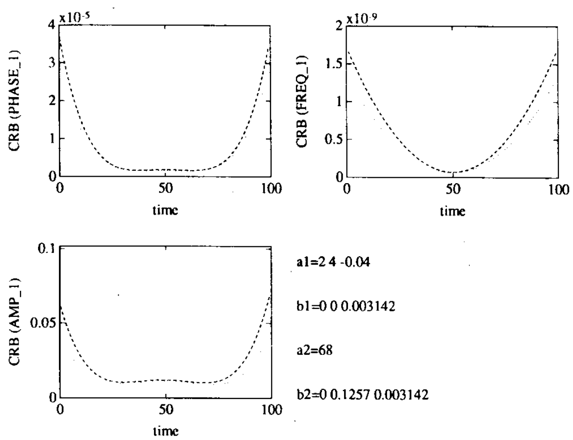

Fig. 2. CRB for the instantaneous phase, frequency, and amplitude of Example 1, component #1, for small difference in the instantaneous frequencies of the two components. The dotted line is the single component case; the dashed line denotes the bound for the same component in the multicomponent case.

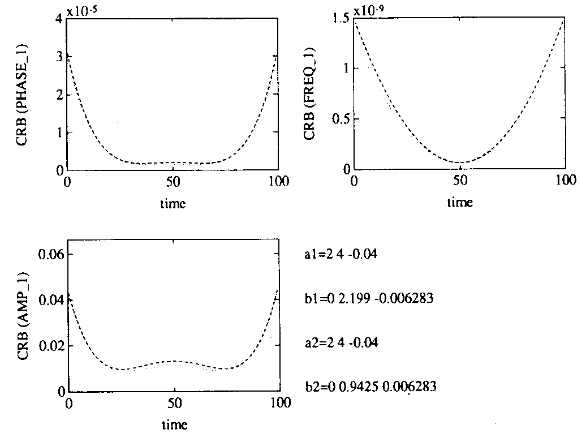

Fig. 3. CRB for the instantaneous phase, frequency, and amplitude of component #1 in Example 2. The multicomponent signal is the sum of two quadratic amplitude crossing chirps.

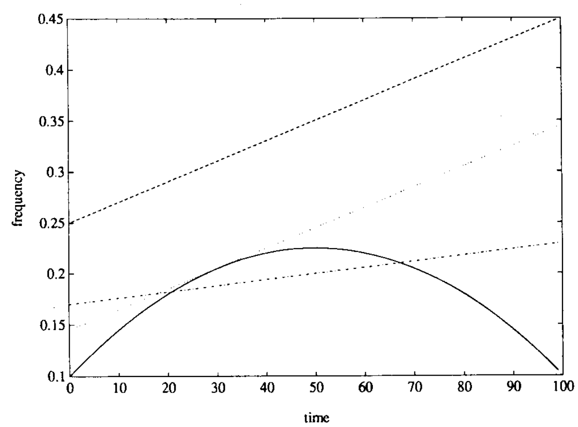

Fig. 4. Instantaneous frequencies of the multicomponent signal in Example 3. The multicomponent signal is the sum of a linear and quadratic chirps, both of constant amplitude. Solid line denotes the instantaneous frequency of the quadratic chirp. The instantaneous frequency of the linear chirp for Case I is denoted by a dashed line; the instantaneous frequency of the linear chirp for Case II is denoted by a dotted line; the instantaneous frequency of the linear chirp for Case III is denoted by a dashed-dotted line.

Component #1 is the same in both. The instantaneous frequency of component #2 is changed from experiment to experiment. In **Case I**, the frequency trajectory of component #2 (dashed line in Fig. 1) is such that the two chirps are well separated. In **Case II**, the frequency trajectory of component #2 (dotted line in Fig. 1), is such that the instantaneous frequencies of the two components are relatively close. The CRB for component #1 in Case II is depicted in Fig. 2. In this section, in all the figures showing CRB's, dotted lines denote the bound for the single component case, while dashed lines denote the bound for the same component in the multicomponent case. Qualitatively similar results are obtained for the second component as well.

As the difference in the instantaneous frequencies of the two components becomes larger (as in Case I), the FIM tends to a block diagonal structure, in which separate diagonal blocks correspond to the amplitude and phase parameters of each component. Hence, when the difference in the instantaneous frequencies of the two components is sufficiently large, in the sense defined below, the CRB's of the different components are essentially decoupled, and therefore, the CRB's are essentially the same as in the single component case (dotted curves in Fig. 2). Therefore, all of the results presented for the single component case hold approximately for each of the multiple components, as long as the components are well separated.

On the other hand, as the difference in the instantaneous frequencies of the two signals decreases, the bounds become higher than in the corresponding single component cases. When the difference approaches zero, the FIM approaches a singular matrix.

Throughout this section, when we talk about frequency differences being small or large, we mean relative to the average instantaneous bandwidth of each of the two components. As was discussed in [1], the ratio of the difference in instantaneous frequencies to the instantaneous bandwidth is an important

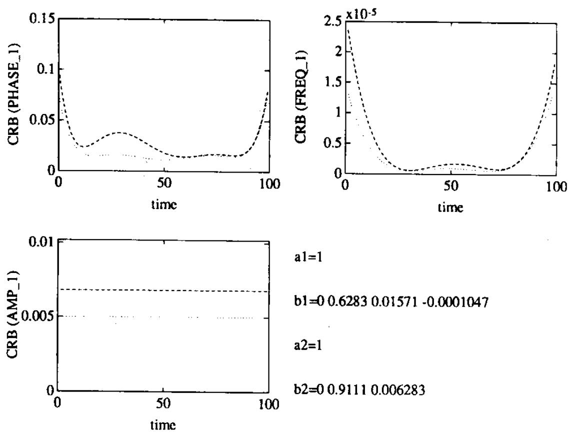

Fig. 5. CRB for the instantaneous phase, frequency, and amplitude of the quadratic chirp component in Case II of Example 3.

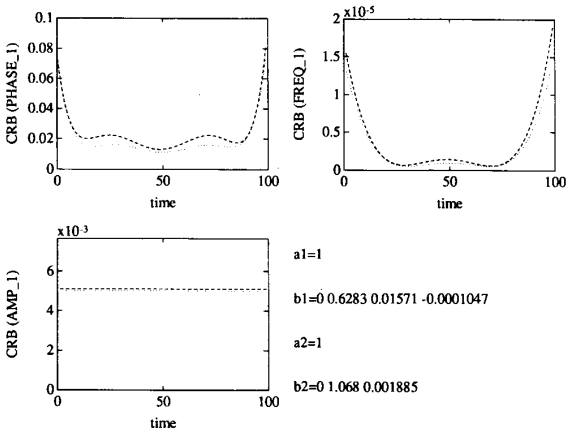

Fig. 6. CRB for the instantaneous phase, frequency, and amplitude of the quadratic chirp component in Case III of Example 3.

quantity when studying multicomponent signals. A meaningful definition of a multicomponent signal requires that this ratio will be larger than unity for each pair of components.

Example 2: This example involves two crossing chirp signals. The two signals amplitudes are second order polynomials. As illustrated by Fig. 3, the bound on the instantaneous phase is getting larger near the crossing time ($t = 50$), relative to its value for the single component signal. On the other hand, at the crossing moment, the bound on the instantaneous frequency is almost identical to its value in the single component case. Since the results for the first and second component are identical, only the results for the first component are presented. Qualitatively similar results are obtained for the case of two constant amplitude crossing chirps.

Example 3: Consider a multicomponent signal comprised of a linear and quadratic chirps, both of constant amplitude. The frequency separation of the frequency trajectories of the signal's two components vary as illustrated in Fig. 4. Three distinct cases are discussed. In all three cases, the quadratic chirp component is the same one. However, the instantaneous frequency of the linear chirp component varies from case to case.

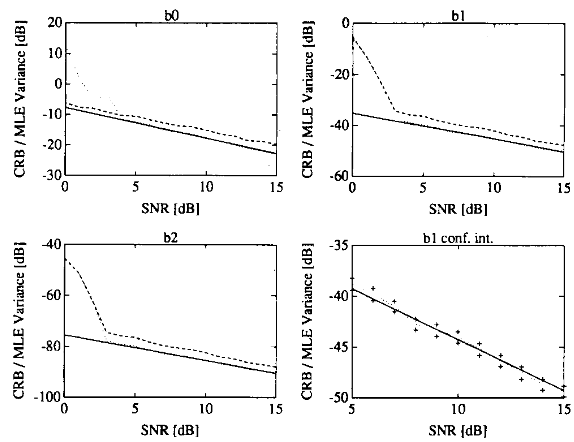

Fig. 7. Estimation performance of phase parameters. Solid lines denote the CRB, dotted lines denote the experimental variance of the ML estimates, and dashed lines denote the variance of the initial estimates. The bottom right figure shows the experimental variance of the ML estimate of b_1, its confidence interval, and the CRB, for high SNR.

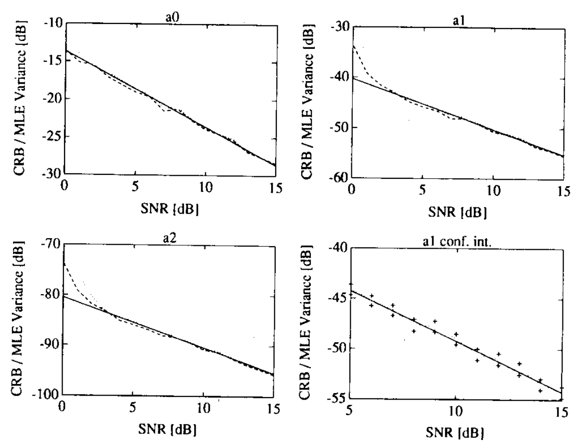

Fig. 8. Estimation performance of amplitude parameters. The bottom right figure shows the experimental variance of the ML estimate of a_1, its confidence interval, and the CRB, for high SNR.

- **Case I:** The frequency trajectories of the linear and quadratic chirps are well separated.
- **Case II:** The frequency trajectories of the linear and quadratic chirps are equal at a single time instant.
- **Case III:** The frequency trajectories of the linear and quadratic chirps cross each other.

The CRB's for the quadratic chirp component in Case II and Case III are depicted in Figs. 5 and 6. In Case I, where the frequency trajectories are well separated, the CRB's of the different components are essentially decoupled, and therefore, the CRB's are essentially the same as in the single component case (dotted curves in Figs. 5 and 6). Note that in both Examples 2 and 3 the frequency bound at the crossing times is almost the same as in the single component case, but the phase bound is away from the single component case. This is due to the fact that at the crossing time, the frequencies of the two components are identical. Hence, at this moment, their sum is a single sinusoid, and its frequency estimation problem is similar to the case of a single sinusoid. On the other hand, the phase signals are identical up to a constant difference. Since the estimation of the two constants strongly depends on the ability to estimate the individual instantaneous amplitudes of the two signals, the bound on the phase at the crossing moment is higher.

B. Performance Example of the ML Algorithm

In this section, we illustrate the performance of the ML algorithm by Monte Carlo simulations. We compare the variance of the estimation errors of the ML algorithm with the CRB and with the variance of the suboptimal algorithm used for initialization. The suboptimal estimation algorithm employs the polynomial phase transform to estimate the phase parameters. This transform assumes that the signal has a constant amplitude. By substituting the phase estimates into (17), we obtain an initial estimate of the amplitude parameters.

Consider a single component signal. Its amplitude and phase are second-order polynomials of time, such that $\boldsymbol{a} = [0.02672, 0.05343, -0.0005343]^T$ and $\boldsymbol{b} = [1.047, 0.06283, 0.0003142]^T$. The amplitude parameters were chosen such that the amplitude energy in the observed time period is equal to 1. The SNR is defined as the ratio of the energy of a constant amplitude signal whose energy equals that of the time varying signal to the noise variance. In the following figures, solid lines denote the CRB, dotted lines denote the experimental variance of the ML estimates, and dashed lines denote the variance of the initial estimates. The experimental plots are based on 500 independent realizations of the signal.

The results depicted in Figs. 7 and 8 show that the ML estimates have a variance essentially equal to the CRB, when the SNR exceeds approximately 3 dB. The initial variances of the phase parameters is about 2–3 dB higher than the CRB. The bottom-right figure in Figs. 7 and 8 shows the experimental variance of the ML estimates of the parameters b_1 and a_1, respectively, the confidence intervals, and the CRB, for the higher SNR's. The results show that the CRB on the variance of the estimated parameters is within the confidence interval of the experimental variance of the ML algorithm. Similar results are obtained for the other parameters and thus illustrate the statistical efficiency of the ML algorithm.

VI. CONCLUSIONS

In this paper, we studied the estimation of signals consisting of one or more components of the form $a(t)e^{j\phi(t)}$, where the amplitude and phase functions are represented by a linear parametric model. We derived the Cramér–Rao lower bound on the error variance in estimating the phase and amplitude parameters as well as the CRB for the instantaneous frequencies of the signal components. A maximum likelihood algorithm for estimating the phase and amplitude parameters was also presented, although it is of secondary importance to this paper, which focuses on performance analysis.

By analyzing the CRB for the single-component case, we have shown that the estimation of the amplitude and the phase are decoupled and that the CRB for the amplitude parameters depends only on the basis functions for the amplitude and is independent of both the amplitude parameter values and of the phase of the signal. Furthermore, the CRB for the phase parameters depends on the amplitude waveform and the basis functions for the phase but does not depend explicitly on either the phase or the choice of the parametric model for the amplitude function.

The results presented here provide a way of analyzing and estimating an important class of nonstationary signals. While current approaches to the analysis of nonstationary signals focus on nonparametric time-frequency distributions, the proposed technique provides an alternative parametric approach.

APPENDIX
COMPUTATION OF $\partial J/\partial \boldsymbol{b}$

The derivative of the objective function $J(\boldsymbol{\theta})$ with respect to $\boldsymbol{b}$ is defined as the following $1 \times \Sigma_{m=1}^{I}(P_m+1)$ row vector:

$$\frac{\partial J(\boldsymbol{\theta})}{\partial \boldsymbol{b}} = \left[\frac{\partial J(\boldsymbol{\theta})}{\partial b_{1,0}}, \cdots, \frac{\partial J(\boldsymbol{\theta})}{\partial b_{I,Q_I}}\right]. \tag{A.1}$$

Using (19), we have

$$\begin{aligned}\frac{\partial J(\boldsymbol{\theta})}{\partial \boldsymbol{b}} &= \tilde{\boldsymbol{y}}^T \frac{\partial \boldsymbol{P}_{\boldsymbol{\Psi}}^{\perp}}{\partial \boldsymbol{b}} \tilde{\boldsymbol{y}} \\ &= \operatorname{tr}\left\{\frac{\partial \boldsymbol{P}_{\boldsymbol{\Psi}}^{\perp}}{\partial \boldsymbol{b}} \boldsymbol{\Gamma}\right\}\end{aligned} \tag{A.2}$$

where $\boldsymbol{\Gamma} = \tilde{\boldsymbol{y}}\tilde{\boldsymbol{y}}^T$. We first evaluate $\partial \boldsymbol{P}_{\boldsymbol{\Psi}}^{\perp}/\partial b_{i,k}$:

$$\begin{aligned}\frac{\partial \boldsymbol{P}_{\boldsymbol{\Psi}}^{\perp}}{\partial b_{i,k}} = -\Bigg\{ &\frac{\partial \boldsymbol{\Psi}}{\partial b_{i,k}} (\boldsymbol{\Psi}^T\boldsymbol{\Psi})^{-1}\boldsymbol{\Psi}^T + \boldsymbol{\Psi}(\boldsymbol{\Psi}^T\boldsymbol{\Psi})^{-1}\frac{\partial \boldsymbol{\Psi}^T}{\partial b_{i,k}} \\ &- \boldsymbol{\Psi}(\boldsymbol{\Psi}^T\boldsymbol{\Psi})^{-1}\left[\boldsymbol{\Psi}^T \frac{\partial \boldsymbol{\Psi}}{\partial b_{i,k}} + \frac{\partial \boldsymbol{\Psi}^T}{\partial b_{i,k}}\boldsymbol{\Psi}\right] \\ &\cdot (\boldsymbol{\Psi}^T\boldsymbol{\Psi})^{-1}\boldsymbol{\Psi}^T\Bigg\}.\end{aligned} \tag{A.3}$$

For notational convenience we define

$$\boldsymbol{R} = \boldsymbol{\Psi}(\boldsymbol{\Psi}^T\boldsymbol{\Psi})^{-1} = [\boldsymbol{r}_1, \cdots, \boldsymbol{r}_I] \tag{A.4}$$

where $\boldsymbol{r}_i$ is a $2(M+1) \times (P_i+1)$ matrix. Note that $\boldsymbol{P}_{\boldsymbol{\Psi}} = \boldsymbol{R}\boldsymbol{\Psi}^T = \boldsymbol{P}_{\boldsymbol{\Psi}}^T$. Inserting (A.3) into (A.2), we get

$$\begin{aligned}\frac{\partial J(\boldsymbol{\theta})}{\partial b_{i,k}} &= -\operatorname{tr}\left\{\frac{\partial \boldsymbol{\Psi}}{\partial b_{i,k}}\boldsymbol{R}^T\boldsymbol{\Gamma}\right\} - \operatorname{tr}\left\{\boldsymbol{R}\frac{\partial \boldsymbol{\Psi}^T}{\partial b_{i,k}}\boldsymbol{\Gamma}\right\} \\ &\quad + \operatorname{tr}\left\{\boldsymbol{R}\boldsymbol{\Psi}^T\frac{\partial \boldsymbol{\Psi}}{\partial b_{i,k}}\boldsymbol{R}^T\boldsymbol{\Gamma}\right\} + \operatorname{tr}\left\{\boldsymbol{R}\frac{\partial \boldsymbol{\Psi}^T}{\partial b_{i,k}}\boldsymbol{\Psi}\boldsymbol{R}^T\boldsymbol{\Gamma}\right\} \\ &= -\operatorname{tr}\left\{\boldsymbol{R}^T\boldsymbol{\Gamma}\frac{\partial \boldsymbol{\Psi}}{\partial b_{i,k}}\right\} - \operatorname{tr}\left\{\boldsymbol{\Gamma}\boldsymbol{R}\frac{\partial \boldsymbol{\Psi}^T}{\partial b_{i,k}}\right\} \\ &\quad + \operatorname{tr}\left\{\boldsymbol{R}^T\boldsymbol{\Gamma}\boldsymbol{P}_{\boldsymbol{\Psi}}\frac{\partial \boldsymbol{\Psi}}{\partial b_{i,k}}\right\} + \operatorname{tr}\left\{\boldsymbol{P}_{\boldsymbol{\Psi}}\boldsymbol{\Gamma}\boldsymbol{R}\frac{\partial \boldsymbol{\Psi}^T}{\partial b_{i,k}}\right\} \\ &= -\operatorname{tr}\left\{\boldsymbol{R}^T\boldsymbol{\Gamma}\boldsymbol{P}_{\boldsymbol{\Psi}}^{\perp}\frac{\partial \boldsymbol{\Psi}}{\partial b_{i,k}}\right\} - \operatorname{tr}\left\{\boldsymbol{P}_{\boldsymbol{\Psi}}^{\perp}\boldsymbol{\Gamma}\boldsymbol{R}\frac{\partial \boldsymbol{\Psi}^T}{\partial b_{i,k}}\right\}.\end{aligned} \tag{A.5}$$

Note that

$$\frac{\partial \boldsymbol{\Psi}}{\partial b_{i,k}} = \left[\mathbf{0}, \cdots, \mathbf{0}, \frac{\partial \boldsymbol{\Psi}_i}{\partial b_{i,k}}, \mathbf{0}, \cdots, \mathbf{0}\right] \tag{A.6}$$

where $\boldsymbol{\Psi}_i = [\mathrm{Re}\{\boldsymbol{\Phi}_i\}^T, \mathrm{Im}\{\boldsymbol{\Phi}_i\}^T]^T$. Therefore

$$\begin{aligned}\frac{\partial J(\boldsymbol{\theta})}{\partial b_{i,k}} &= -\,\mathrm{tr}\left\{\boldsymbol{r}_i^T \boldsymbol{\Gamma} \boldsymbol{P}_{\boldsymbol{\Psi}}^{\perp} \frac{\partial \boldsymbol{\Psi}_i}{\partial b_{i,k}}\right\} - \mathrm{tr}\left\{\boldsymbol{P}_{\boldsymbol{\Psi}}^{\perp} \boldsymbol{\Gamma} \boldsymbol{r}_i \frac{\partial \boldsymbol{\Psi}_i^T}{\partial b_{i,k}}\right\} \\ &= -\,2 \cdot \mathrm{tr}\left\{\boldsymbol{r}_i^T \boldsymbol{\Gamma} \boldsymbol{P}_{\boldsymbol{\Psi}}^{\perp} \frac{\partial \boldsymbol{\Psi}_i}{\partial b_{i,k}}\right\} \\ &= -\,2 \cdot \tilde{\boldsymbol{y}}^T \boldsymbol{P}_{\boldsymbol{\Psi}}^{\perp} \frac{\partial \boldsymbol{\Psi}_i}{\partial b_{i,k}} \boldsymbol{r}_i^T \tilde{\boldsymbol{y}}. \end{aligned} \tag{A.7}$$

The second equality follows from the fact that

$$\begin{aligned}\mathrm{tr}\left\{\boldsymbol{P}_{\boldsymbol{\Psi}}^{\perp} \boldsymbol{\Gamma} \boldsymbol{r}_i \frac{\partial \boldsymbol{\Psi}_i^T}{\partial b_{i,k}}\right\} &= \mathrm{tr}\left\{\frac{\partial \boldsymbol{\Psi}_i}{\partial b_{i,k}} \boldsymbol{r}_i^T \boldsymbol{\Gamma} \boldsymbol{P}_{\boldsymbol{\Psi}}^{\perp}\right\} \\ &= \mathrm{tr}\left\{\boldsymbol{r}_i^T \boldsymbol{\Gamma} \boldsymbol{P}_{\boldsymbol{\Psi}}^{\perp} \frac{\partial \boldsymbol{\Psi}_i}{\partial b_{i,k}}\right\}. \end{aligned} \tag{A.8}$$

Let

$$\tilde{\boldsymbol{b}}_{i,k} = \frac{\partial \boldsymbol{\Psi}_i}{\partial b_{i,k}} \boldsymbol{r}_i^T \tilde{\boldsymbol{y}}, \qquad k = 0 \cdots Q_i, \qquad i = 1 \cdots I \tag{A.9}$$

$$\boldsymbol{B}_i = [\tilde{\boldsymbol{b}}_{i,0}, \tilde{\boldsymbol{b}}_{i,1}, \cdots, \tilde{\boldsymbol{b}}_{i,Q_i}], \qquad i = 1, \cdots, I. \tag{A.10}$$

Using these notations, the derivative of the objective function with respect to the phase parameters of the ith signal is given by

$$\begin{aligned}\frac{\partial J(\boldsymbol{\theta})}{\partial \boldsymbol{b}_i} &= \left[\frac{\partial J(\boldsymbol{\theta})}{\partial b_{i,0}}, \cdots, \frac{\partial J(\boldsymbol{\theta})}{\partial b_{i,Q_i}}\right] \\ &= -\,2 \cdot \tilde{\boldsymbol{y}}^T \boldsymbol{P}_{\boldsymbol{\Psi}}^{\perp} \boldsymbol{B}_i. \end{aligned} \tag{A.11}$$

Now let

$$\overline{\boldsymbol{B}} = [\boldsymbol{B}_1, \cdots, \boldsymbol{B}_I]. \tag{A.12}$$

Using (A.12) we finally obtain

$$\frac{\partial J(\boldsymbol{\theta})}{\partial \boldsymbol{b}} = -2 \cdot \tilde{\boldsymbol{y}}^T \boldsymbol{P}_{\boldsymbol{\Psi}}^{\perp} \overline{\boldsymbol{B}}. \tag{A.13}$$

In the special case where both the amplitude and phase basis functions are polynomials, the computation of the above expressions can be considerably simplified by defining

$$\overline{\boldsymbol{\Phi}}_i = j \cdot [e^{j\phi_i(\boldsymbol{t})}, \boldsymbol{t}e^{j\phi_i(\boldsymbol{t})}, \boldsymbol{t}^2 e^{j\phi_i(\boldsymbol{t})}, \cdots, \boldsymbol{t}^{P_i+Q_i} e^{j\phi_i(\boldsymbol{t})}]. \tag{A.14}$$

Then, $\boldsymbol{B}_i$ can be written as

$$\boldsymbol{B}_i = \overline{\boldsymbol{\Psi}}_i \overline{\boldsymbol{R}}_i \tag{A.15}$$

where

$$\overline{\boldsymbol{\Psi}}_i = \begin{bmatrix} \mathrm{Re}\{\overline{\boldsymbol{\Phi}}_i\} \\ \mathrm{Im}\{\overline{\boldsymbol{\Phi}}_i\} \end{bmatrix} \tag{A.16}$$

and

$$\overline{\boldsymbol{R}}_i = \begin{bmatrix} \boldsymbol{r}_i^T \tilde{\boldsymbol{y}} & 0 & \cdots & 0 \\ 0 & \boldsymbol{r}_i^T \tilde{\boldsymbol{y}} & & 0 \\ \vdots & & \ddots & \vdots \\ 0 & 0 & & \boldsymbol{r}_i^T \tilde{\boldsymbol{y}} \end{bmatrix} \tag{A.17}$$

is a $(P_i + Q_i + 1) \times (Q_i + 1)$ matrix.

In this case, the derivative of the objective function with respect to the phase parameters of the ith signal is given by

$$\frac{\partial J(\boldsymbol{\theta})}{\partial \boldsymbol{b}_i} = -2 \cdot \tilde{\boldsymbol{y}}^T \boldsymbol{P}_{\boldsymbol{\Psi}}^{\perp} \overline{\boldsymbol{\Psi}}_i \overline{\boldsymbol{R}}_i. \tag{A.18}$$

REFERENCES

[1] L. Cohen, "What is a multicomponent signal," in *Proc. Int. Conf. Acoust., Speech Signal Processing*, 1992, pp. V-113–V-116.

[2] ——, "Time-frequency distributions—A review," *Proc. IEEE*, vol. 77, no. 7, pp. 941–981, July 1989.

[3] F. Hlawatsch and G. F. Boudreaux-Bartels, "Linear and quadratic time-frequency signal representation," *IEEE Signal Processing Mag.*, pp. 21–67, Apr. 1992.

[4] B. Boashash, "Estimating and interpreting the instantaneous frequency of a signal—Part 1: Fundamentals," *Proc. IEEE*, vol. 80, no. 4, pp. 539–568.

[5] B. Boashash, Ed., *New Methods in Time frequency Analysis*. Sydney, Australia: Longman Chesire, 1992.

[6] S. Peleg and B. Porat, "The Cramér-Rao lower bound for signals with constant amplitude and polynomial phase," *IEEE Trans. Signal Processing*, vol. 39, pp. 749–752, Mar. 1991.

[7] ——, "Estimation and classification of polynomial-phase signals," *IEEE Trans. Inform. Theory*, vol. 37, pp. 422–430, Mar. 1991.

[8] S. Peleg and B. Friedlander, "A technique for estimation the parameters of multiple polynomial phase signals," presented at 1992 Symp. Time-Frequency Time-Scale Anal., Victoria, Canada, Oct. 4–6, 1992.

[9] S. Peleg, "Estimation and detection with the discrete polynomial transform," Ph.D. dissertation, Dept. Elec. Comput. Eng., Univ. of California, Davis, CA, 1993.

[10] R. Kumaresan and S. Verma, "On estimating the parameters of chirp signals using rank reduction techniques," in *Proc. Twenty-First Asilomar Conf. Signals, Syst., Comput.*, Nov. 1987, pp. 555–558.

[11] R. M. Liang and K. S. Arun, "Parameter estimation for superimposed chirp signals," *Proc. 1992 ICASSP*, San Francisco, CA, Mar. 23–27, 1992.

[12] G. H. Golub and V. Pereyra, "The differentiation of pseudo-inverse and nonlinear least square problems whose variables separate," *SIAM J. Numer. Anal.*, vol. 10, pp. 413–432, Apr. 1973.

[13] M. R. Osborne, "Some special nonlinear least square problems," *SIAM J. Numer. Anal.*, vol. 12, pp. 571–592, Sept. 1975.

[14] D. G. Luenberger, *Linear and Nonlinear Programming*. Reading, MA: Addison-Wesley, 1984, 2nd ed.

[15] R. Fletcher, *Practical Methods of Optimization: Vol. I—Unconstrained Optimization*. New York: Wiley, 1980.

[16] S. Zacks, *The Theory of Statistical Inference*. New York: Wiley, 1971.

[17] C. R. Rao, *Linear Statistical Inference and Its Applications*. New York: Wiley, 1965.

[18] B. Friedlander, "Parametric signal analysis using the polynomial phase transform," in *Proc. IEEE Signal Processing Workshop Higher Order Statistics*, June 7–9, 1993, Stanford Sierra Camp, South Lake Tahoe.

Benjamin Friedlander (S'74–M'76–SM'82–F'87) received the B.Sc. and M.Sc. degrees in electrical engineering from the Technion-Israel Institute of Technology in 1968 and 1972, respectively, and the Ph.D. degree in electrical engineering and the M.Sc. degree in statistics from Stanford University in 1976.

From 1976 to 1985, he was at Systems Control Technology, Inc., Palo Alto, CA. From November 1985 to July 1988, he was with Saxpy Computer Corporation, Sunnyvale, CA. Currently, he is with the University of California at Davis and Signal Processing Technology, Ltd. in Palo Alto, CA.

Dr. Friedlander is the recipient of the 1983 ASSP Senior Award, the 1985 Award for the Best Paper of the Year from the European Association for Signal Processing (EURASIP), and the 1989 Technical Achievement Award of the Signal Processing Society.

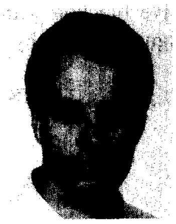

Joseph M. Francos (S'89–M'90) was born on November 6, 1959 in Tel-Aviv, Israel. He received the B.Sc. degree in computer engineering in 1982 and the D.Sc. degree in electrical engineering in 1990, both from the Technion-Israel Institute of Technology, Haifa.

From 1982 to 1987, he was with the Signal Corps Research Laboratories, Israeli Defense Forces. From 1991 to 1992, he was with the Department of Electrical Computer and Systems Engineering at the Rensselaer Polytechnic Institute as a Visiting Assistant Professor. He then was with the MIT Media Laboratory during the summer of 1992. During 1993, he was with Signal Processing Technology, Palo Alto, CA. In 1993, he joined the Department of Electrical and Computer Engineering, Ben-Gurion University, Beer-Sheva, Israel, where he is now a Lecturer. His current research interests are in parametric modeling and estimation of 2-D random fields, random fields theory, parametric modeling and estimation of nonstationary signals, image modeling, and texture analysis and synthesis.